ELECTRICAL RESISTIVITY TOMOGRAPHY AND MAGNETIC SURVEYS: APPLICATIONS FOR BUILDING SITE CHARACTERIZATION AT GUBRE, WOLKITE UNIVERSITY SITE, WESTERN ETHIOPIA

Tigistu Haile [1] and Alemayehu Ayele [2]

[1] School of Earth Sciences, College of Natural Sciences, Addis Ababa University, P O Box 1176, Addis Ababa, Ethiopia. E-mail: htigistu@yahoo.com
[2] Department of Geology, Arba Minch University, P O Box 21, Arba Minch, Ethiopia

ABSTRACT: A study aimed at evaluating the competence of the near surface formations as foundation materials has been undertaken at the site of the newly established Wolkite University Campus. Integrated geophysical surveys involving 2D Electrical Resistivity Tomography (ERT), Vertical Electrical Sounding (VES) and magnetic surveys have been used for the purpose. The ERT and VES results show the presence of intermediate to low resistivity top soil, an even lower resistivity second layer of clay and/or high moisture content underlain by weathered and fresh bedrocks, and a number of vertical or near vertical discontinuities and weak zones in the site. The magnetic anomaly plots, have mapped the weak zones resulting from subsurface structures and the Euler depth map and 2D magnetic modelling specially depicting the depth of the magnetic sources that are associated with the bedrock. The correlation of the magnetic anomaly plot and 2D inverse model resistivity sections are used for the identification of weak zones that need special building design consideration at the site. The work emphasizes the viability of high resolution electrical tomographic surveys in engineering site investigations to augment geotechnical investigations that depend on data from a limited number of points to characterize large areas and complex geologic settings.

Key words/phrases: Building foundation, electrical resistivity tomography, Euler deconvolution, magnetic anomaly, slice-stacked section

INTRODUCTION

Examination of the engineering geological properties of soils and rocks for geotechnical investigations require borings and/or sampling in a close-order grid. These investigations provide information on the physical or mechanical and chemical properties of rocks and soils that are relevant to the design of a foundation for proposed structures. Other important aspects to be obtained from such studies are the depth of the building foundations and the presence of any irregularities of the subsurface revealed during excavation. Yet one commonly accepts geotechnical data from a limited number of data points to characterize large areas and complex geologic settings (Benson, 1993). The extrapolation/interpolation of the results obtained from the limited number of tests, however, is not representative over a larger area due to inhomogeniety of the subsurface materials. In addition to this, the probable existence of active faults, failure surfaces, underground cavities, lateral transition of geological formations in locations otherwise untouched with the geotechnical boreholes are missed with the study. In order to obtain sufficiently complete picture of site conditions, measurements must be taken over denser spacing than direct samplings are normally done. This generally incurs higher costs and makes the geotechnical methods inhibitive.

Geophysical techniques which can be taken with denser measurement spacing than direct sampling and involve much less costs, however, are potentially useful in characterizing building sites with adequate accuracy when large sites are to be studied. These methods are able to investigate and determine parameters and subsurface characteristics such as soil properties, bedrock depth and its topography below unconsolidated material, rock type, layer boundaries, water table depth and presence of weak zones and expansive clays. Furthermore, these investigations provide information on inhomogeneities of the subsurface, presence of cavities, ancient relics and generally underground structures or bodies that have different physical

properties from their geological surroundings (Aubert, 1984).

Geophysical and geotechnical results could then be combined to ascertain the in-situ properties of the subsurface. Engineering geophysics combined with geotechnical engineering focus on the behaviour and performance of soils and rocks in the design and construction of civil, environmental and mining engineering structures. The two methods are often the most cost-effective and rapid means of obtaining subsurface information, especially when the area involved is large (Soupios, 2007; Soupios *et al.*, 2007; Oyedele and Bankole, 2009).

In the present study, a combination of surface geophysical investigation techniques (2-D electrical resistivity imaging, Vertical Electrical Sounding (VES) and magnetic surveying) are used to characterize a building site and determine its suitability for building foundations. The methods were employed to determine the subsurface electrical stratification, the presence of structures like weak zones and faults, contact between lithologic units and the depth to the

possible foundation bedrock and its undulation/morphology.

MATERIALS AND METHODS

The study area

The study area, the Wolkite University campus, is located at the western margin of the Main Ethiopian Rift (MER) valley which forms/is part of the East African Rift System (EARS) that runs from northeast to southwest almost dissecting Ethiopia into two parts. The site is located in the Southern Nations, Nationalities and Peoples Regional State (SNNPS) along the main asphalt road of Addis Ababa-Wolkite and on a detour all weather gravel road of Wolkite-Gubre, 158 km from Addis Ababa. More specifically, the site is situated about 12km from Wolkite town and at a place called Gubre (location 37° 47' 60E long, 8° 11'60N lat, elevation 1931 m) whose location is shown in Figure 1. The investigated site is bounded by geographical coordinates of 37°32'30'' to 38°07'00'' east and 8°19''30''to 8°25'15'' north.
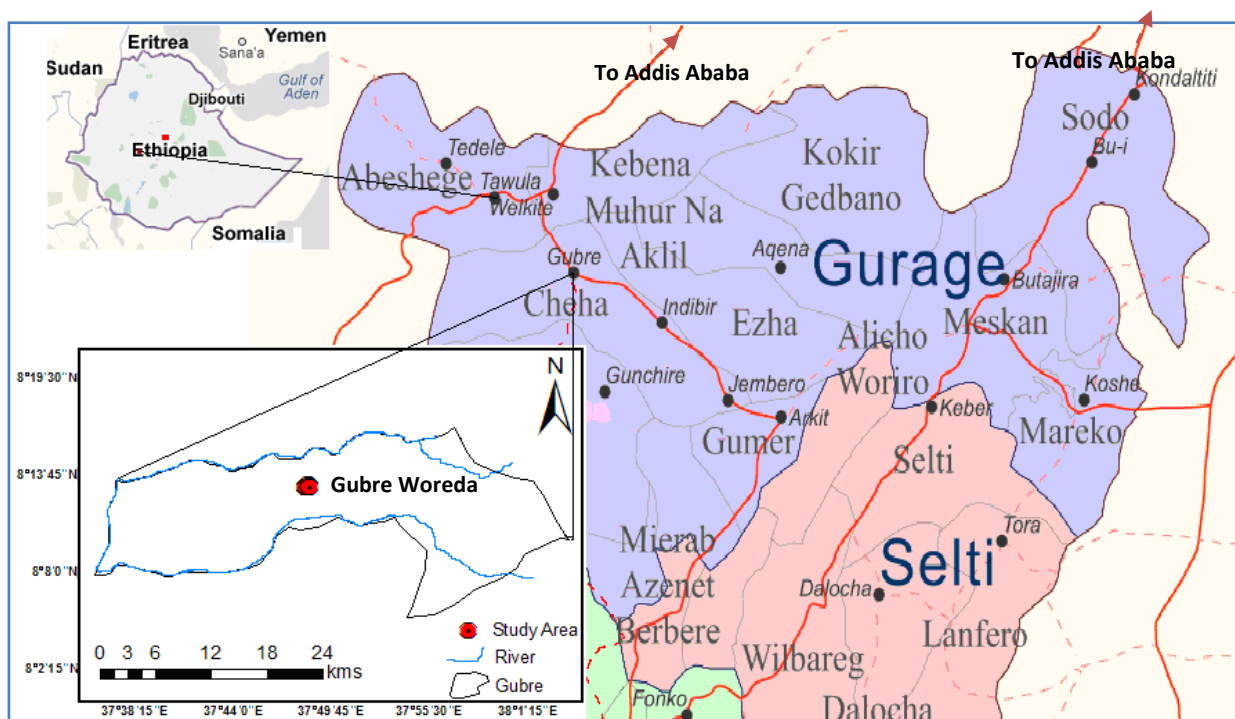

Figure 1. Location map of the study area within Gurage Administrative Zone.

Methodology, instruments and data

The Electrical Resistivity Tomography/Imaging (ERT) Technique

A number of surface geophysical methods can be used for the purpose of geotechnical site investigation out of which the electrical resistivity method has found increasing application. The greatest limitation of the most widely used of the electrical surveying field setups- the resistivity sounding (VES) method- however, is that it does not take into account lateral changes in layer resistivity (Kearney *et al.*, 2002). The effect of such lateral changes can result in errors in the interpreted layer resistivity and/or thickness. In many engineering and environmental studies, the subsurface geology is very complex where the resistivity can change rapidly over short distances. The 1-D resistivity sounding method may not thus be sufficiently accurate for such situations (Loke, 2000).

Such shortcomings are overcome with a new developed concept of Electrical Imaging or Electrical Resistivity Tomography (ERT) that is widely being used in resistivity instrumentation and data acquisition to map areas with moderately complex geology where conventional sounding or profiling surveys are inadequate (Griffiths and Barker, 1993; Loke and Barker, 1996; Loke, 1997; 1999). The technique has appeared to make the acquisition of many readings in a minimized amount of time possible and has been found to be specifically appropriate for engineering and environmental applications corresponding to shallow investigation- depths with the order of 10 to 80m. The technique has an added attraction of providing a relatively low cost, non-invasive and rapid means of generating 2D models of the geoelectrical properties of the subsurface (Robert and William, 1981; Bell, 1983).

The concept involves applying multi-core cables which contain as many individual wires as the number of electrodes, with one take-out every 5m, 10m, and a set of 24, 48, 72, 96 electrode layouts. The measurement includes the use of a sequence of readings uploaded on to the units' internal memory. The goal of this unit is to take automatic readings for many combinations of transmission and reception pairs, consequently achieving some kind of mixed profiling and sounding pairs (ABEM, 2004). The total length of the cable is the multiplication of electrode/-pickup spacing by the number of electrodes and that determines the depth of investigation of the setup as well (Loke, 2001; Bernard, 2003).

One technique used to horizontally extend the area covered by the survey, particularly for a system with a limited number of electrodes, is the roll-along method. After completing the measurements with the initial setup- the main sequence- the cable is shifted past to one end of the line (roll along sequence) by several unit electrodes spacing. Hence, a set of sequences that include the main and roll along sequences were used to obtain, in the particular system used for this work, 648 data points from the main sequences and 297 data points from the roll along sequence thus establishing the large data density and high resolution claim of the imaging technique.

The 2D electrical resistivity imaging (ERT), vertical electrical sounding (VES) and magnetic data in this study were collected along a number of selected profiles. The traverses for the ERT surveys consisted of four lines- three parallel profiles (Profiles– 1, 2 and 3) and one perpendicular profile (Profile–4)- with a total surveyed length of about 1.5 km (Fig. 2). An inter-electrode spacing of 3 m was used which, with the 72 electrode IRIS setup, gives nominal depth of investigation of 35 m, more than adequate for most building site characterization. VES data were obtained from three sounding points spaced at about 50 m on Profile–2 with maximum half current electrode spacing of 220 m (Fig. 2).

The other geophysical method used in the study is the ground magnetic survey. The relevance of the magnetic method in mapping subsurface structures, discontinuities and weak zones find wide application in engineering and geotechnical investigations (Thomas, 2003). The method is routinely employed for subsurface study to outline geological structures which might cause unsafe conditions in building foundation. In this case the techniques developed for deeper applications (such as mining, geothermal and crustal studies), are scaled for shallow targets by moving to shorter wavelength/higher frequencies. Merely scaling a deep investigation tool with respect to frequency, to adapt it to near-surface investigations is, however, insufficient, when looking for spatial variations in near-surface geology, it is also important to increase

the spatial sampling density and thus reduce aliasing (Pellerin, 2002; Hansen *et al.*, 2005).

What we have done in this work is therefore to acquire an increased number of data points (high data volume) and also consider the higher frequency components of the magnetic signal, the last of which is achieved through the use of interpretation software (Thompson, 1982; Reid, 1990; Benson, 1993; Miller and Singh, 1994; Thomas, 2003; Salem *et al.*, 2007).

The magnetic data were collected over the ERT profiles and over random points well distributed to cover the area of investigation. Measuring station spacing's between 20 to 30 m has been used. The total magnetic data collected during the field survey (excluding base station readings) was 152 data points while 150 data were used for the interpretation. The survey traverses are depicted in Figure 3.

The instruments used for the survey included the IRIS instruments Syscal R1 Plus Switch 72 IP and Resistivity unit, for both the tomographic and VES surveys- in "multielectrode" and "Rho" modes, respectively, and the Scintrex IGS-2 proton precision magnetometer in "total field" mode

for the magnetic surveys. A Global Positioning System (Garmin, 2007) was used to record position locations and timings of series of discrete magnetic reading measurements.

Geology of the study area

The Ethiopian Rift is covered with Cenozoic volcanics and Tertiary and Quaternary sediments except the appearance of patchy Precambrian rocks. The volcanic rocks are dominantly fissural basaltic lava flows, rhyolites and ignimbrites associated with volcano-clastic tuff and ash deposits (Mohr, 1967). Older volcanic units (Pre-Pliocene) outcrop on the rift escarpment or margin and recent volcanics cover the entire rift floor (Kazmin, 1981).

The Main Ethiopian Rift (MER), close to which the investigation site is located, contains abundant acidic lavas and ignimbrites which are associated with central volcanoes containing wide calderas. Quaternary central volcanic products cover the axial rift. On the MER, per-alkaline silicic ignimbrites, unwelded pyroclastics and minor lavas related to fissural eruptions of regional extent are the most abundant volcanic rocks (Tenalem Ayenew *et al.*, 2008).
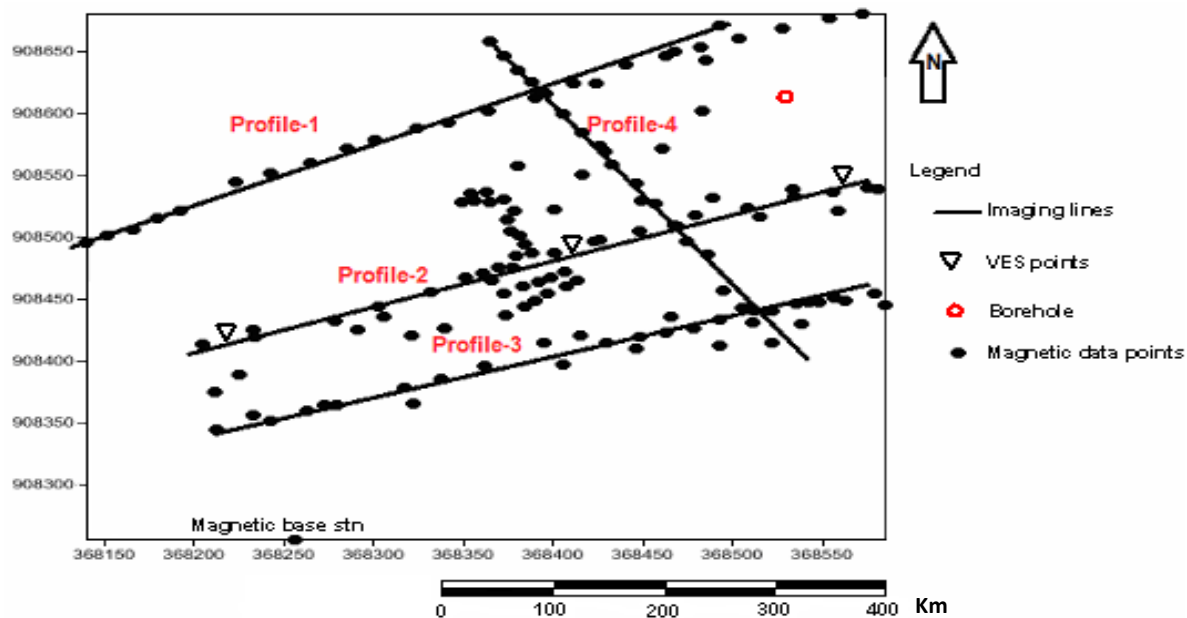

Figure 2. Electrical imaging survey traverses (solid lines), VES points (inverted triangles) and magnetic survey data points (solid dots). Only representative magnetic data points are shown to avoid congestion of the plot. Geographic coordinates in UTM.

When considering regional structures, the rift floor and its escarpments are highly faulted. The faults in the MER are parallel and sub-parallel to the NE–SW trending rift axis (Giday Woldegebriel *et al.*, 1990). The Rift floor is affected by several faults that form smaller horst and graben structures. The NNE-SSW and N-S trending faults are the dominant faults (Kazmin, 1980).

Geology of the study area and its surroundings

The general geologic setup of the study area and its surroundings, which are located close to the western margin of the Main Ethiopian Rift, is as given in Figure 3. The following are the important lithostratigraphic units of the area (Merla *et al.*, 1979; Kazmin, 1981; Seifemichael Berhe *et al.*, 1987; Mengesha Tefera *et al.*, 1996; Dereje Ayalew *et al.*, 2006 and the references therein; Efrem Beshawered, 2010):

Jimma Lower Basalts*:* This unit is the oldest and most extensive flood basalt over the region. It usually forms flat lying plateaus, often tilted and for the most part, is horizontally stratified. In outcrop, the rock unit is partly weathered; fine grained or apahanitic with no phenocrysts. Microscopically, it is composed of 60% plagioclase, 30% pyroxene, 8% opaque and 2% olivine with intergranular and intersertal texture.

Jimma Upper Basalts: This unit is found on the southwest of the study area. In hand specimen, it is dark-grey in color, medium to coarse grained and hard and compact in appearance in fresh samples, but reddish brown in weathered ones. Microscopically, it is composed of 50% plagioclase, 20% pyroxene, 15% opaques and 15% olivine. It shows intergranular and intersertal texture.

Tarmaber-Megezez Formation: This unit is found in the central, west and northern portion of the mapped area. It is transitional to alkali basalt with large aerial coverage and is composed of plagioclase, pyroxene, and opaque minerals. It is dark grey in fresh samples, but reddish brown in weathered specimens.

Welded to Partially Welded Pyroclastic Flows: This unit belongs to one of the Nazareth group (Tsegaye Abebe *et al.*, 2005; Efrem Beshawered, 2010). It is light to dark-grey in fresh samples and reddish to yellow to pink in weathered ones. It is fine grained, densely welded rock containing vitrophyric fiamme and lithic fragments with associated rhyolitic lava flows revealed with ash and unwelded tuffs. Microscopically, it consists of crystals of 35% K-feldspar (sanidine), 40% quartz, 20% plagioclase and 5% hornblende having vitrophyric texture.

At a local scale, the site is covered by thick recent sediment deposits expect at river cut and road exposures. Cenozoic volcanic rocks and thick recent residual deposits characterize the study area. Local geologic setup of the study area was described based on the observations of river cut, road section, bore holes and pitting. Lithological units of the study site are basalt, rhyolite, ignimbrite, tuff, volcanic ash and residual soils.

Basalt: This rock unit is exposed in the western side of the study area along river cut and road exposure. It is black in color in fresh samples and of light gray colour in weathered expousers. It is aphanitic in texture.

Rhyolite: This rock unit is exposed in the western side of the University site along river cut and road exposure. It is characterized by reddish weathered and light colour. It is a fine grained and strong rock unit.

Ignimbrite: It is welded tuff and a special group of pyroclastic rocks. It exposed along river cut and road exposure. This unit is located in the western portion of the study area and exhibits light colour and forms flat to near steep slopes.

Tuff: This pyroclastic unit is exposed in the eastern, western and southern portion of the study area along river cut and road section. It is characterized by white color and fine-grained texture. The tuff unit of the study area is relatively soft and porous that is usually formed by welding the compaction and cementation of volcanic ash.

Volcanic ash: It is a pyroclastic material exposed in the western side of the construction sites. The volcanic ash consists of powder size to sand-size particles of igneous rock material that have been blown into the air by an erupting volcano and deposited on the ground as ash fall deposit. It is characterized by light-gray colour and insoluble in water.
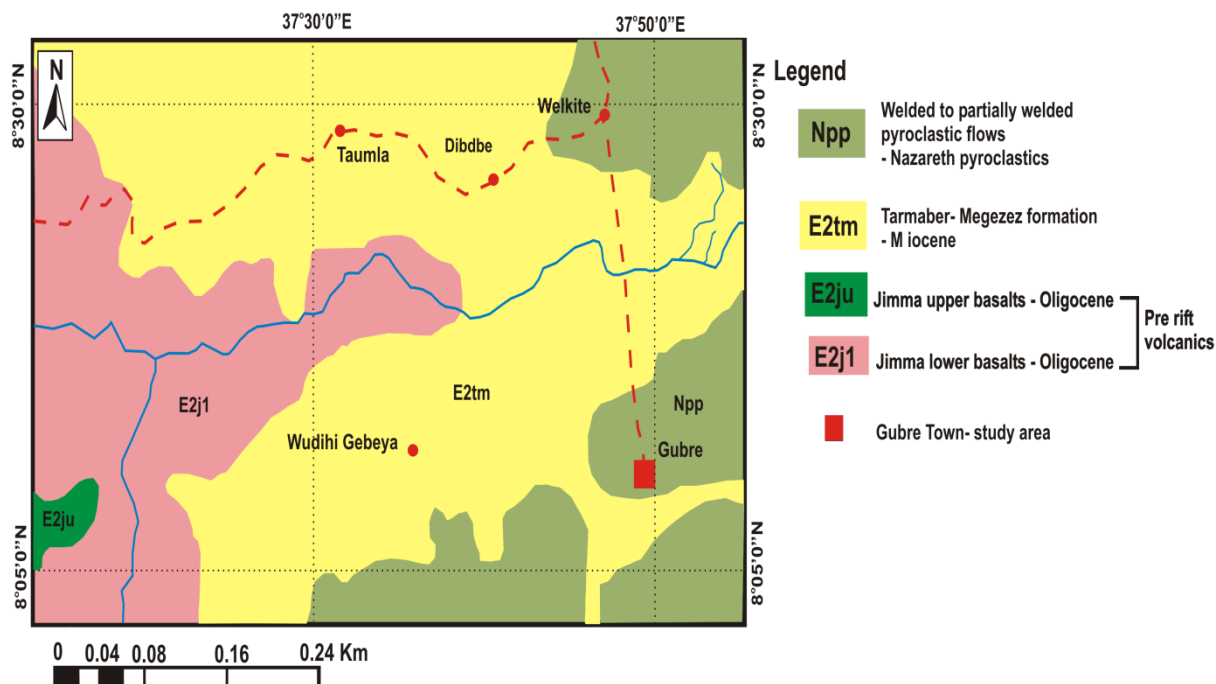
Figure 3. Geological map of the study area and its surroundings (after Efrem Beshawered, 2010).

Residual deposits: This unit covers almost all of the study area. Residual soil is the soil that remains at the place of their formation. The upper portion of the deposit in the study area is totally altered into black cotton clay and silt soil. Thick soil deposit, reaching to a depth of 5 m, is observed at the central portion of the study area.

DATA PROCESSING

Imaging data pre-processed through automatic filtering of the ProsysII software and visual inspection and preferential removal of noisy data was finally processed with the RES2DINV software (Geotomo, 2006) to obtain the inverse model resistivity sections that give a high resolution 2D image of the subsurface. The quality of match between the filtered raw data and model calculated apparent resistivity values, indicated by a Root Mean Square (RMS) error parameter, for the present study, ranged from 2.4 to 6.9% with acceptable number of iterations, showing a good data quality.

A sliced-stacked pseudo-depth section map, derived from sliced apparent resistivity sections, was further used for a better understanding of the subsurface condition of the whole survey area. This map can show the entire picture of the subsurface of survey area and

enables an overall examination of the site in view of its suitability for building foundation.

For the VES surveys on the other hand, the layer parameters of the individual VES are obtained using the 1D inversion of the WinResist Software. The interpreted parameters of the three VES are used to construct the 2D geoelectric section of the subsurface along Profile–2.

The magnetic data were corrected for diurnal variation and removal of unwanted/unacceptable instrumental readings through close examination of the data. IGRF determined values of 2005 (IGRF, 2010) were used to reduce the resulting data to the magnetic anomalies. As the study area is found within the low latitude magnetic equator and covers a very small area, latitude and longitude correction were insignificant and not done. In addition to this, in magnetic equatorial regions where inclination is less than 15 degrees, reduction to the pole is generally unstable and cannot be derived (Geotech, 2007). Due to this reason reduction to the pole was not also done.

For the electrical data, the spatial geophysical mapping and modelling has been assisted using a suite of software such as Electre II, PROSYS II, RES2DINV, GEOSOFT, Geosoft Oasis Montaj v. 6.4.2, Surfer 9.11, WinResist, RESIX-IP and AutoCAD 2007 softwares. On the other hand, with the corrected magnetic data, plotting and enhancement techniques were used to obtain magnetic anom-

aly, analytical signal, tilt derivative and Euler deconvolution maps that were used for interpretation. The corrected data was also used in 2D modelling for Profile–2.

INTERPRETATION

Electrical resistivity 2D *imaging and magnetic profiles*

During the present study, interpretation of the geophysical data has been carried out to give a meaningful geological interpretation and examine the suitability of the construction site for building foundation. In contrast to routine geotechnical investigations that give data from discrete points, the electrical resistivity imaging survey especially gives a 2-D picture of the subsurface that delivered continuous information, greater depth of investigation and bridge the discontinuous and confined information of the subsurface obtained from the geotechnical data.

Additional borehole data (from the Ewan borehole close to the site) helped to understand the vertical geological section of the study area and to correlate the different units with the 2-D electrical imaging and geoelectric sections. The depth of the borehole used for lithological correlation is 18m; whereas the depths of the electrical resistivity imaging and geoelectric sections are nominally about 39.4 and 45m respectively- therefore correlation between the well lithologic log and the inaging section was done only up to the corresponding depths. A geoelectric section was developed for Profile–2 to validate the 2D imaging data.

In the following sections, interpretation of the electrical and magnetic data for each survey profile is done separately.

Parallel profiles– 1, 2 and 3

These three profiles run almost parallel to each other and are oriented in a near southwest-north east direction. By joining main sequences and number of rolls along sequences, the profiles have covered surveyed lengths of 378m, 432m and 378m respectively. The number of data points used to construct the inverse model resistivity sections after initial filtering and removal of noisy data are 1471 for Profile–1, 1774 data points for Profile–2 and 1478 data points for Profile–3. The data points used in the inversion process show the high density data of the

imaging survey and form the basis for the claimed high resolution of the imaging technique. The inversion result shows good quality raw data with RMS error of 6.9%, 3.2% and 6.4% attained after only 4 and 5 iterations for Profiles–1, 2 and 3, respectively.

For the purpose of correlation with the electrical data, the corrected magnetic data values picked up from the corresponding profiles are plotted as profile plots on top of each model. These are given in Figure 4.

From the inverse model resistivity sections it is seen that the subsurface can be divided into three/four distinct layers. A top layer of intermediate resistivity (6 to 16 Ω-m) corresponding to the top soil of dark clay and sandy silt with average thickness of about 3 to 6 m. This is followed by a low resistivity (1.1 to 3.8 Ω-m) layer corresponding to the presence of higher moisture content on soil pore spaces and/or higher clay content (wet clay) of average thickness of 7 m. This second layer is underlain by a thin region of intermediate resistivity nearly similar in response to the first layer and having an average thickness of about 3 m. It is a layer of highly weathered and fractured ignimbrite.

The substratum mapped in the survey is a high resistivity horizon which, from the point of view of the objective of the survey, can be considered as a single unit which is extensive over the area both laterally and in depth forming the competent bed rock. Within this extensive layer of high resistivity, however, are blocks of relatively high weathering resistant earth materials interspersed with a number of vertical/near vertical low resistivity zones that are the responses of subsurface discontinuities or weak zones. The identification of these week zones on the various profiles, which could not otherwise be detected from point geotechnical data are the important results of this work.

On the right side of Figure 4(b) is shown the correlation between Ewan Well with the inverse model resistivity section for the corresponding depths between the well and the model section. For the corresponding depths, the correlation depicts a relatively low resistivity top soil that matches with the dark clay and yellow sandy silt soils, a very low resistivity zone that correlates with the clay layer and the high resistivity horizons with weathered and fractured ignimbrite
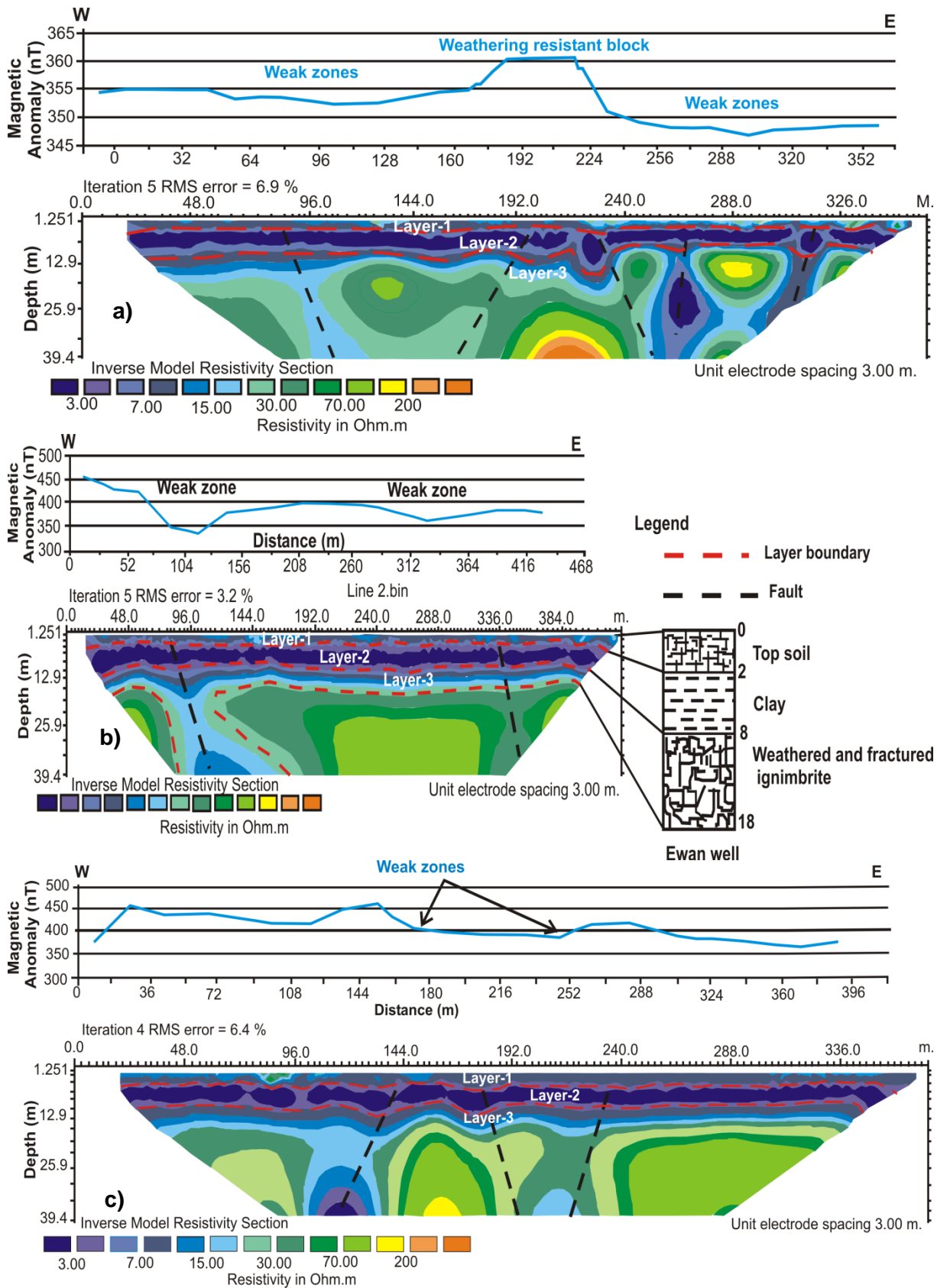
▲

Figure 4. a, b, and c. Combined interpretations of magnetic anomaly and 2D electrical resistivity imaging inverse model sections for Profiles– 1, 2 and 3 respectively and correlation with lithologic log of the Ewan Well in (b) (Note the remarkable correlation between the magnetic profile plots and the resistivity model sections in depicting the weak zones).

The corresponding magnetic anomaly profile plots along the 2D electrical imaging of Profiles–1, 2 and 3 are also as shown in the top sections of each figure. Two features dominate these profile plots- the very high magnetic anomalies that resulted from the relatively highly magnetized weathering resistant blocks, and low magnetic anomalies corresponding to the low magnetization weathered material filled sections and areas of change in slopes of the plots which are indicative of lithological contacts/weak zones. What is apparent here is the remarkable correspondence between the electrical data and the magnetic profile plots in depicting these weak zone and the bed rock responses.

Profile–4

This profile was chosen to run nearly perpendicular to other three profiles and is basically intended to map the presence (if any) of structures oriented parallel to three profiles and would otherwise be missed by them. The profile length is about 270 m and 850 data points have been used in the inversion attaining an RMS error of 2.4% after just 5 iterations showing again good data quality.

The inverse model resistivity section (Fig. 5) shows four distinct layers. The resistivity variation from the section is almost identical (up to 19m) with the results obtained from the other three perpendicular profiles in that a top layer of relatively low resistivity zone (dark clay and yellow sandy silt soil) followed by a low resistivity intermediate layer (clay layer), followed by a layer of relatively higher resistivity value (fractured and weathered ignimbrite) and finally a higher resistivity substratum (the bed rock in the area) are mapped from top to bottom.

A positive correlation in terms of depicting the subsurface features is observed between the inverse resistivity model section with that of the corresponding magnetic plot, which shows significant amplitude variation in magnetic signature. One observes strong maxima on either end of the profile resulting from the response of the bed rock with a wide minimum in the middle section resulting from the intervening structure/weak zone. Correlation with the Ewan Well is also given up to the depth where the lithologic log of the well corresponds with depth of the imaging section (Fig. 5).

Vertical Electrical Sounding Surveys

Vertical electrical sounding surveys have also been carried out with the Shlumberger expanding spread on Profile–2 to examine the deeper electrical stratification of the subsurface over the construction site. Three VES have been conducted. An illustration of a typical sounding curve and its interpreted parameters with 1D inversion is given in Figure 6. The geoelectric section constructed from interpretation of the three VES and which depicts the electrical stratification of the subsurface over the area is given in Figure 7(a).
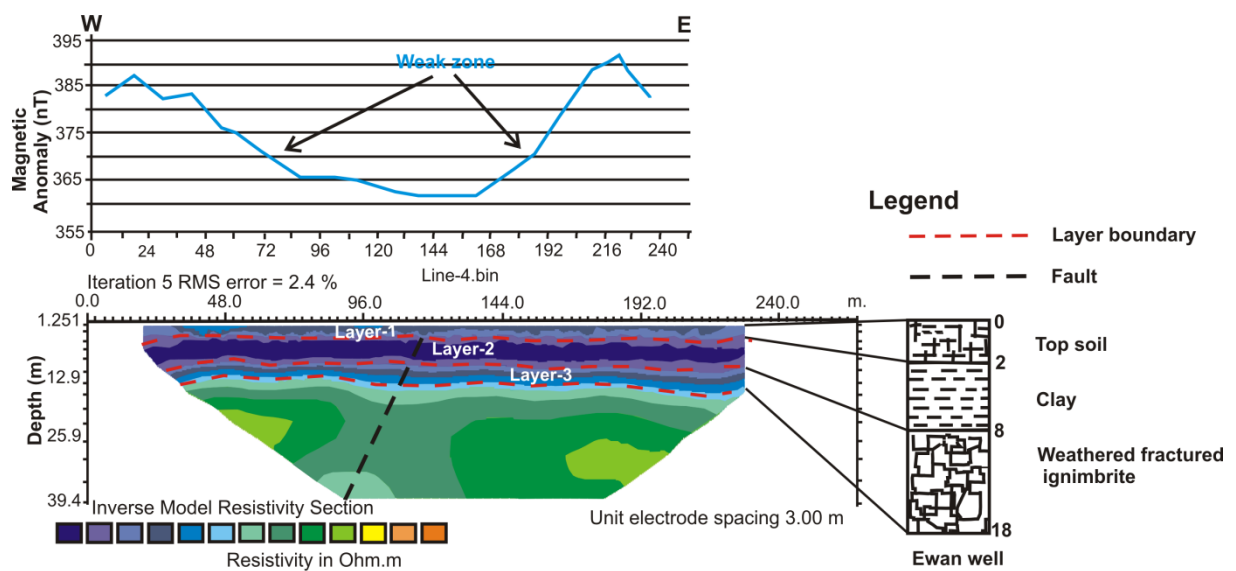

Figure 5. Combined interpretations of magnetic anomaly and 2D electrical resistivity imaging along Profile–4.
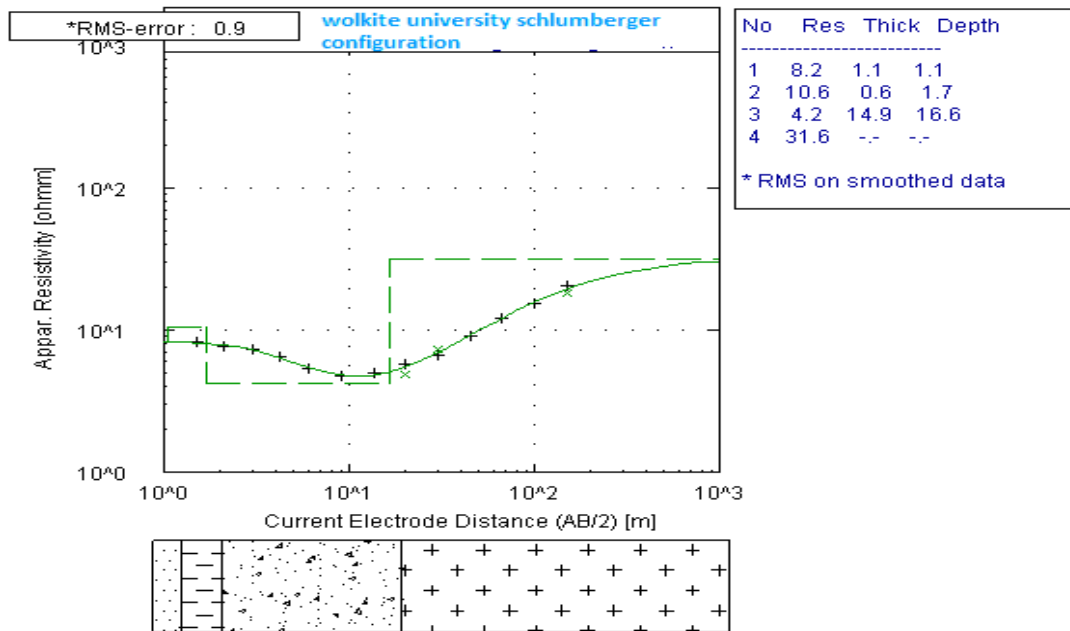
Figure 6. Typical 1D interpretation of VES (VES-1, Profile–2), and geological interpretation.

The first layer is the top dry soil which is composed of dark clay and yellow sandy silt soil that shows relatively low resistivity ranging from 2–15.2Ω-m and extending to a depth of 2 m. The second layer in the geoelectric section exhibits very low resistivity values that could be due to clay soil and/or because of higher moisture content relative to the overlying layer. From the geo-electric section, the resistivity of this layer is seen to vary from 3.25 to 4.5Ω-m and its depth extends to 17 m. This layer increases in thickness from the eastern side of the traverse to the western side. The resistivity values of the third layer are in the range of 26-32.1Ω-m. This relatively higher resistivity response could be due to the weathered fractured ignimbrite.

The magnetic 2D profile model for Profile–2 was developed from the data picked from the analytical signal map and is given in Figure 7(b). This profile plot shows significant amplitude variation in the magnetic anomaly signatures. This plot is also believed to characterise the current site and its suitability for building foundation. The modelled layers reveal sharp contacts/peak maxima at two locations i.e., at distances of 144m and 290m. This is due to occurrence of high magnetic susceptibility materials relative to the surrounding. The curves further exhibit minima at the distance of 100m and 200 m with a value of 400nT, which can be interpreted as the signature of the weak zones depicted in the inverse model resistivity sections. There certainly is a positive correlation between the magnetic anomaly plots with 2D electrical profile sections in detecting the concealed weak zones. The good fit between the magnetic anomaly plot and the 2D electrical imaging inverse model sections as well as the geo-electric section increase the certainty in the identification of weak zones that potentially pose a hazard or need special design consideration for the building foundation.

Stacked apparent resistivity psuedosection map

It is essential to view synoptically both the vertical and lateral variation of electrical resistivity over the area to understand the general geological framework. This is conveniently achieved through the construction of a sliced-stacked map from the resistivity values picked up from the imaging data carried out on the profiles. When the sliced depth sections are arranged in stacked plot form, they provide a simple image that depicts the whole picture of the subsurface of the investigated area.
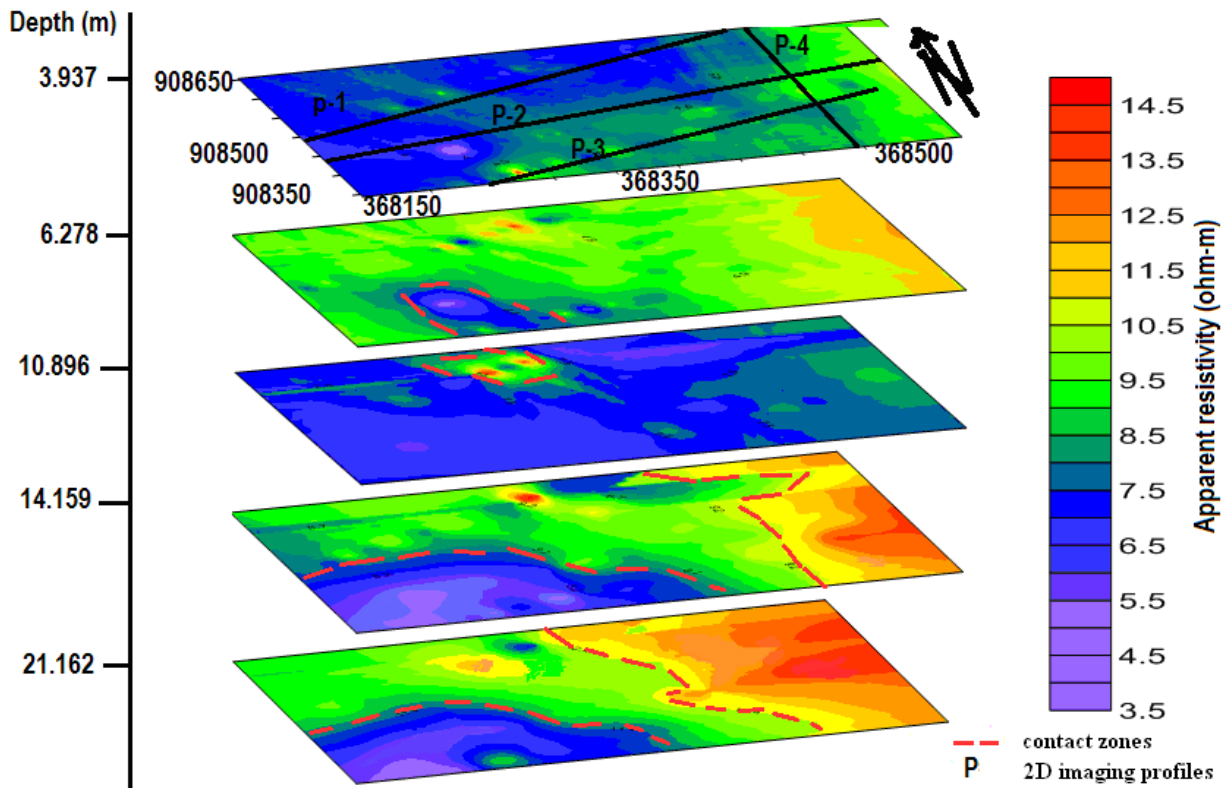
Figure 7. (a) Geoelectric section, and (b) Magnetic 2D model section along Profile–2.

An apparent resistivity sliced-stacked depth map is prepared (Fig. 8) from the 2D electrical resistivity imaging data of the four profiles at five different depth levels to enable one to visualize the whole surveyed area in terms of the distribution of resistivity regimes.

From the sliced-depth and stacked plot shown in Figure 8, it is possible to preferentially divide the whole subsurface into three zones: a very low resistivity zone, most likely the response of recent sediment deposits which cover most parts of the survey area. This low resistivity disappears for the most part at a depth of about 6.278 m but reappears and extends downward to depths greater than 10.896 m.

A second zone is distinguished from other zones by having intermediate resistivity which ranges from 8 to 11Ω-m. This zone is extensive over the survey area at depth beyond 6.278 m and, as compared to the first; the coverage of this zone increases from depth greater than 14.159 m.

A third zone is characterized by higher resistivity values 11.5-15Ω-m. This zone is widely distributed on the eastern part of the survey area. Analogous to the second zone, the coverage of this zone increases at depth greater than 14.159 m. In summary, from the stacked resistivity pseudodepth section map, depth to bedrock is relatively shallower at the eastern part of the survey area. As result, this part of the study area is suitable for sitting large size buildings as there is a reduced risk from foundation settling and soil consolidation.

Figure 8. Sliced-Stacked Apparent resistivity pseudo-section map of the entire study area.

Magnetic anomaly map

The magnetic anomaly map of the study area is shown in Figure 9(a). From the anomaly plot, the mapped area can be categorized into four parts represented by zones A, B, and C corresponding to different range of values in the anomaly signature. Zone A, which is found in the central and north eastern part of the surveyed area, shows very low magnetic anomaly relative to the other regions and it is the region where the subsurface rock units are highly affected by the presence of thick soil cover and/or the presence of weak zones filled with weathered material. This zone is distributed in central part of the study area.

Zone B which covers a large portion of the survey area is characterized by intermediate magnetic anomaly response and is due to moderately weathered and fractured rock units. Zone C depicts regions of very high magnetic anomaly response resulting from the presence of highly magnetized bodies that result from the fresh ignimbrites found at a relatively shallower depth.

This zone covers the western, southern and south-western parts of the construction site. This region is a preferential location for sitting buildings. The map clearly shows the areas of contact between the different units.

Analytical signal map

The analytical signal map shown in Figure 9(b) was developed from the magnetic anomaly map. Over the causative bodies, the analytic signal has a form that depends on the locations of the bodies but not their directions of magnetization. Therefore, this method is very useful at low magnetic latitudes. The map specifically resolves near surface (shallow) anomaly sources very well and is good at locating the edges of shallow bodies, for the reason that the amplitude of the simple analytical signal peaks (attains maxima) over magnetic contacts. Distinct areas associated with geological contacts that need special design consideration for heavy structures are clearly identified and outlined on the map.
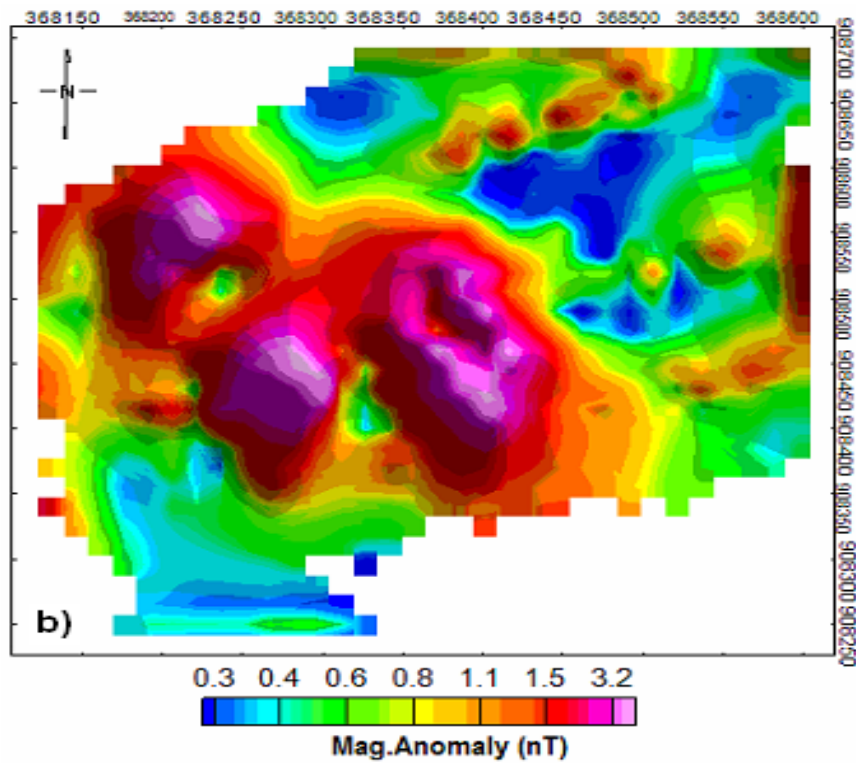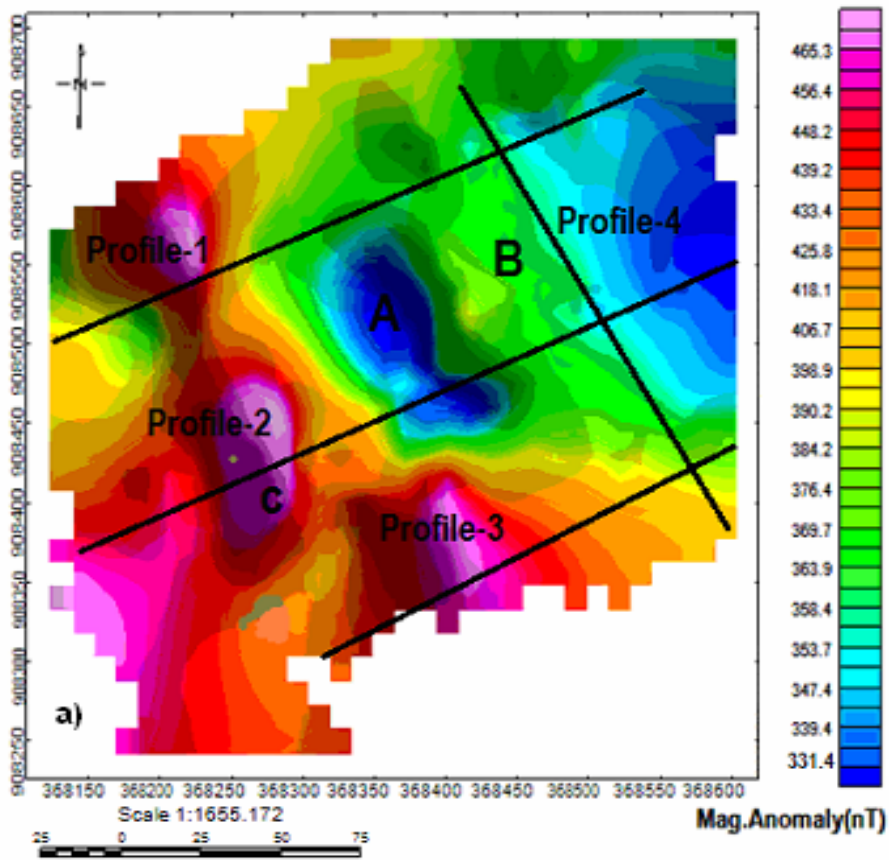
Figure 9. Magnetic Anomaly (a) and Analytical Signal Map (b).

Tilt Derivative of Analytical Signal Map

From the Analytical Signal Map again it is also possible to create the Tilt Derivative Map as shown in the Figure 10 (a). The tilt angle has the attractive property of being positive over sources, cross through zero at or near the edge of a vertical sided source and is negative outside the source region (Miller and Singh, 1994). The tilt derivative of the reduced-to-pole fields have anomaly zero-crossings located close to the edges of structures. The tilt angle overcomes the problem of the shallow and deep sources by dealing with the ratio of the vertical derivative to the horizontal derivative.

Salem *et al.* (2007), has shown that half-distance between +45 and -45 contours provide an estimate of the source depth for vertical contacts. The tilt derivative will be relatively insensitive to the depth of the source and should resolve shallow and deep sources equally well. The tilt derivative method not only estimates the source location and depth but it is also able to resolve sources at different depths.

On Figure 10 (a) the areas that reveal positive over sources cross at/near the edge of a vertical sided source and negative far from the source region are clearly shown. The geological contacts/edges are obviously outlined on the map. Therefore, from the point of view of the magnetic surveys, the areas that show positive over sources and zero at the edges exhibit low bearing capacity due to weathering and fracturing of the rocks while those areas on the map with negative far from the source are characterized by competent rocks of potentially high bearing capacity.

Euler deconvolution

The Euler deconvolution method uses the first order derivative to determine the magnetic sources and estimate their depths, but it requires an assumption about the nature of the source or structural index (Blakely, 1995). If (x_o, y_o, z_o) is the position of a magnetic source whose total field f is measured at (x, y, z) and the total field has a regional value of **B**, then the Euler's equation reduces to:

$$(x - x_0)\frac{\partial f}{\partial x} + (y - y_0)\frac{\partial f}{\partial y} + (z - z_0)\frac{\partial f}{\partial z} = N(B - T)$$

where,
(x_o, y_o, z_o) is the position of a source whose total field *f* is detected at any point (x,y,z),
B is the background value of the total field (T), and N is the degree of homogeneity.

The degree of homogeneity N is interpreted as a structural index (SI) (Thompson, 1982; Reid, 1990) which represents the source type and is a measure of the rate of change of the field with distance. The user must choose the structural index that best fits the data. The choice of a proper structural index is crucial in order to attain correct depths and converging solutions over magnetic contacts. An index that is too low gives depths that are too shallow, and an index that is too high gives estimates that are too deep. The correct index for a particular feature gives the best solution clustering and consequently the best depth estimates.

For the current study, Euler deconvolution for different structural indices and window sizes were used (0, 1, 1.5, 2, 2.5,3 and 3.5) to estimate the depth and magnetic sources for characterizing the building foundation site. Among the structural indices that best fits the data was 2. The resulting Euler depth map shown in Figure 10(b) depicts there is high clustering of solutions at different depths in the north, south and southwest flank than the southeast flank. This has been interpreted as being due to existence of structures (weak zones) that contain highly magnetized bodies in the north, south and south-west flank than the southeast flank. As result, it is recommendable that relatively north-south and south-east flank is high bearing capacity than south- west flank from the engineering point of view.

DISCUSSION

The correlation of inverse model resistivity sections of Profiles– 1, 2 and 3 with the Ewan well lithologic log showed that both represent almost similar features. The layers with relatively higher resistivity values characterize competent strata with good bearing capacity. Thus, the weathered bedrock, which has shown relatively higher resistivity responses, possesses good bearing capacity in comparison to the upper layers of top soil (dark clayey and yellow sandy silty soils) which have lower resistivity responses. The layers with high resistivity response represent fresh bedrock with excellent bearing capacity but such layers were observed at a greater depth. Water bearing formations and the static groundwater level in the area is found at greater depth and has no signifi cant effect on the suitability of the site for buildings, particularly of low rise shallow foundation buildings.
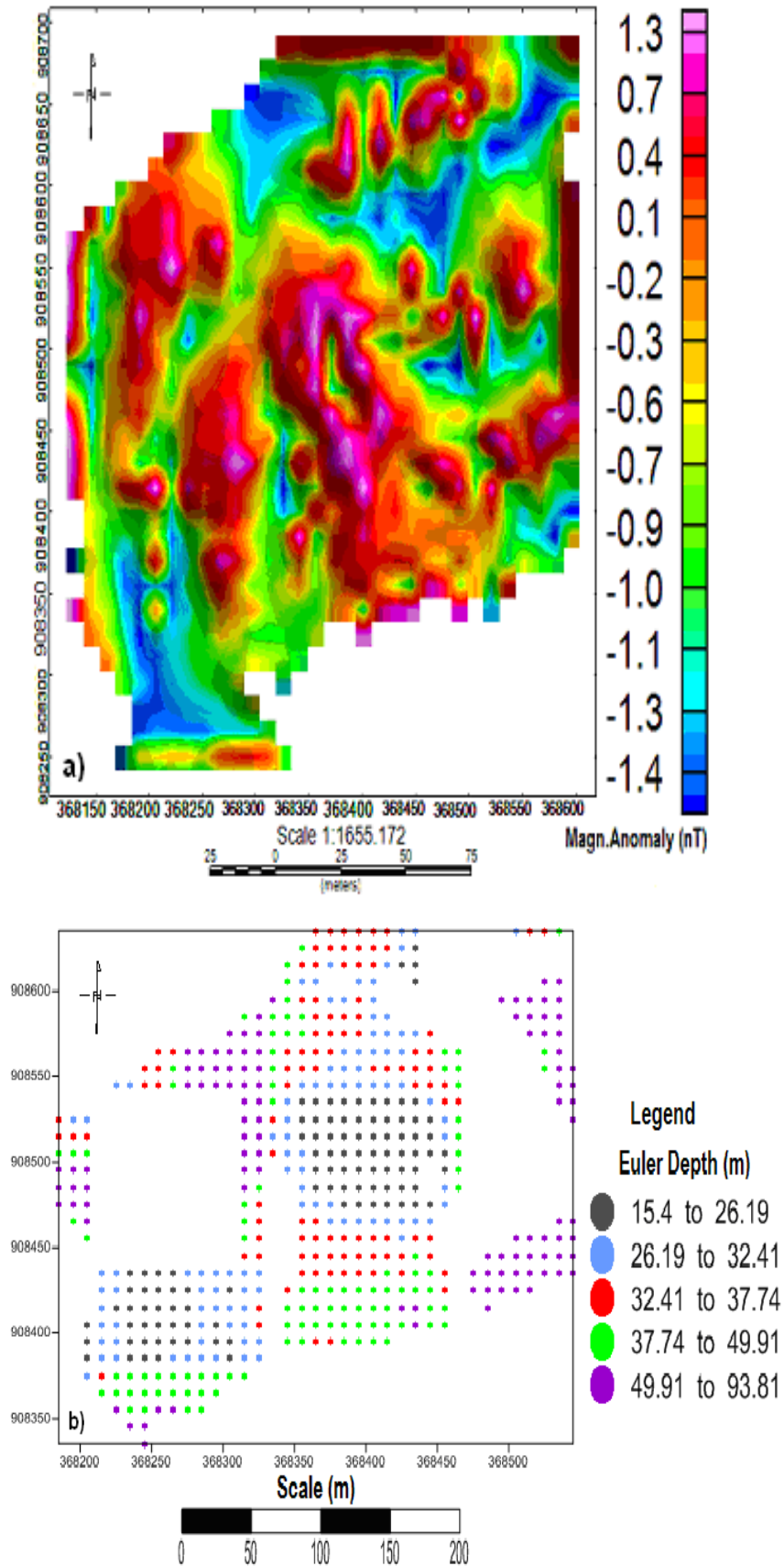
Figure 10(a). Tilt Derivative of Analytical Signal Map and (b) Euler Deconvolution depth map.

Based on the geophysical investigations, it has been observed that the material at shallow depth is mainly clayey and silty soil. Thus, proper estimation of bearing capacity of this relatively poor foundation material is required so that adequate building foundation can be designed. The apparent resistivity pseudo-section shows low resistivity section that exhibit poor bearing capacity at the top part and high resistivity section that exhibit high bearing capacity at greater depth.

The stacked apparent resistivity section indicates that the eastern portions of the study area may provide better bearing capacity for building foundation than the western portion. Further, it is also expected that the strata with low resistivity whose response is potentially a result of higher moisture content/water saturation may possess corrosive potential that may severely affect the steel structures in building foundation. While designing the footing for proposed buildings, therefore, proper care must be taken to protect it from the possible corrosive effect within strata of low resistivity.

From the magnetic anomaly map it may be deduced that high magnetic anomaly contrasts are the result of fresh igneous rocks whereas, low magnetic anomaly contrasts are the responses from weak zones and high degree of weathering in rocks. The analytical signal map clearly identified and outlined distinct areas associated with geological contacts that need special design especially for heavy structures. In addition to these, the tilt derivative of analytic signal map also revealed geological contacts/edges of lithologic units/that one needs to consider during the design of structures. Euler deconvolution and 2D magnetic modelling have shown the depth of magnetic sources associated with the competent units/ the bed rocks.

CONCLUSIONS

The geophysical survey techniques employed in this work have mapped the stratification of the subsurface from their electrical and magnetic responses. As attested through correlation with the lithologic log from a nearby borehole, the methods have mapped the different subsurface layers with a very good resolution. The methods additionally give a 'synoptic view' of the building site and enable the identification of specific

areas of subsurface weakness/discontinuity to be considered during building foundation design. The depth to the competent bed rock over the survey site and its morphology are also mapped.

The work illustrates the viability of, specially, the high resolution electrical resistivity imaging technique to characterise a building foundation site with very good accuracy. Weak zones and subsurface discontinuities that in most instances are missed by geotechnical data (that rely on extrapolation/interpolation of point data) are clearly recognized with the techniques. The geotechnical point data can be combined with the large-coverage and lower cost geophysical data to get an overall sound picture of a building foundation condition, especially when large area construction sites are involved.

REFERENCES

1. ABEM (2004). SAS 4000/SAS 1000 Terrameter instruction manual, 50 pp.
2. Aubert, M. (1984). Resistivity and magnetic surveys in ground-water prospecting in volcanic areas- case history Maar of Beanit, Puy de Dome, France. *Geophysical Prospecting* **32**:554–563.
3. Bell, F.G. (1983). *Fundamentals of Engineering Geology*. Butterworth and Co. Ltd, London, 648 pp.
4. Benson, R.C. (1993). Geophysical techniques for subsurface site characterization. Chapter 14. **In**: *Geotechnical Practice for Waste Disposal*, pp 311–357, (David Daniel, ed.), Chapman and Hall, New York.
5. Bernard, J. (2003). Short notes on the principles of geophysical methods for groundwater investigation at www.Terraplus.com.
6. Blakely, R.J. (1995). *Potential Theory in Gravity and Magnetic Applications*. Cambridge University Press, Australia.
7. CBDSC (2010). Geotechnical investigation of Wolkite University site (report). Construction Building Design Share Company (CBDSC) Addis Ababa, Ethiopia.
8. Construction Building Design Share Company, CBDSC (2010).Geotechnical Investigation of Wolkite University Site, Addis Ababa, Ethiopia, a report
9. Dereje Ayalew, Marty, B., Barbey, P., Gezahegn Yirgu and Endale Ketefo (2006). Sub-lithospheric source for Quaternary alkaline Tepi shield, southwest Ethiopia. *Geochemical Journal* **40**:47–56.
10. Ephrem Beshawered (2010). *Geology of the Akaki-Beseka Area*, Basic Geosciences Mapping Core

process, Geological Survey of Ethiopia. Addis Ababa, Ethiopia.

11. Garmin (2007). Garmin eTrex' HC Series, Personal Navigator Owner's Manual, Garmin Corporation, 48 pp.

12. Geotomo Software (2006). *RES2DINV Ver. 3.55*, Rapid 2-D Resistivity and IP inversion using the least-squares method at http://www.geoelectrical.com. Accessed on June 10, 2012.

13. Geotech (2007). Advanced Processing and Interpretation of Gravity and Magnetic Data at http://www.getech.com. Accessed on June 7, 2012.

14. Giday Woldegabriel, Aronson, J. and Walter, R.C. (1990). Geology, geochronology and rift basin development in the central sector of the Main Ethiopian Rift. *Geol. Soc. Amer. Bult.* **102:**439–458.

15. Griffiths, D.H. and Barker, R.D. (1993). Two-dimensional resistivity imaging and modelling in areas of complex geology. *Applied Geophysics* **29**:211–226.

16. Hansen, R.O., Racic, L. and Grauch V.J.S. (2005). Near Surface Geophysics: Chapter 6, *Magnetic Methods in Near Surface Geophysics,* pp 151–171, (Dwain K. B., ed.) Society of Exploration Geophysicists.

17. IGRF (2010). IGRF model field 11th Generation, online calculator. (IGRF) International Geomagnetic Reference Field. Available at: http://www.ngdc.noaa.gov/IAGA/vmod/igrf.html

18. Kazmin, V. (1980). Transform Faults in the East African Rift system, Geodynamic Evolution of the Afro-Arabian Rift System.

19. Kazmin, V. (1981). *Geological Map of the Ethiopian Rift.* Addis Ababa, Ethiopia.

20. Kearney, P. Brooks, M. and Hill, I. (2002). *An Introduction to Geophysical Exploration,* 3rd ed., Blackwell Science Ltd., 160 pp.

21. Loke, M.H. (2001*). Electrical Imaging Survey for Environmental and Engineering Studies:* A practical guide to 2D and 3D surveys.

22. Loke, M.H. (2000). *Electrical Imaging Survey for Environmental and Engineering Studies:* A practical guide to 2D and 3D surveys, pp 2–4, Penang, Malaysia.

23. Loke, M.H. (1999). *Electrical Imaging Survey for Environmental and Engineering Studies.* A practical guide to 2-D and 3-D surveys, Penang, Malaysia, 57 pp.

24. Loke, M.H. (1997). Electrical imaging surveys for environmental and engineering studies: a practical guide to 2D and 3D surveys: Unpublished short training course lecture notes, University of Sains Malaysia, Penang, Malaysia.

25. Loke, M.H. and Barker R.D. (1996). Rapid least squares inversion of apparent resistivity pseudo-section by a quasi Newton method. *Geophysical prospecting* **44**:131–152.

26. Merela, G., Abbate, E., Azzuroli, A., Bruni, P., Canuti, P., Fazzouli, M., Saari, M. and Tacconi, P. (1979). *Explanation of the Geological Map of Ethiopia and Somalia with the Major Landforms.* Consiglio Nazionale delle Ricerche, Firenze.

27. Miller H.G. and Singh V. (1994). Potential field tilt, a new concept for location of potential sources *Applied Geophysics* **32**:213–217.

28. Mohr, P.A. (1967). The Ethiopian Rift System, *Bulletin of Geophysical Observatory.* Addis Ababa. **11**:1–65.

29. Oyedele, K.F. and Bankole, O.O. (2009). Subsurface stratigraphic mapping using geophysics and its impact on urbanization development in Arepo area, Ogun state, Nigeria. *Science Journal* **2**(2):31–45.

30. Pellerin, L. (2002) Applications of electrical and electromagnetic methods for environmental and geotechnical investigations. *Surveys in Geophysics* **23**:101–132.

31. Reid A.B. (1990). Magnetic interpretations in three dimensions using Euler deconvolution. *Geophysics* **55**:80–91.

32. Robert, D.H. and William, D.K. (1981). *An Introduction to Geotechnical Engineering.* Prentice Hall, Englewood Cliffs, New Jersey, USA.

33. Salem, A. Williams, S., Fairhead, J.D., Ravat, D. and Smith, R. (2007). Tilt-depth method: a simple depth estimation method using first-order magnetic derivatives. *The Leading Edge* **26**(12):1502–1505.

34. Seifemichael Berhe, Belay Desta, Nicoletti, M. and Mengesha Tefera (1987). Geology, geochronology and geodynamic implications of the Cenozoic magmatic province in W and SE Ethiopia. *Journal Geological Society London* **144**:213–226.

35. Soupios, P. (2007). Reconstructing former urban environments by combining geophysical electrical methods and geotechnical investigations. *Geophys. Eng.* **5**:186–194.

36. Soupios, P., Georgakopoulos, P., Papadopoulos, N., Saltas, V., Andreadakis, A., Vallianatos, F., Sarris, A. and Makris, J.P. (2007). Use of engineering geophysics to investigate a site for a building foundation. *Journal of Geophysics and Engineering* **4**(1):94–103.

37. Tenalem Ayenew, Molla Demlie and Wohnlich, S. (2008). Hydrogeological framework and

occurrence of ground water in the Ethiopian Aquifers. *Journal of African Earth Science* **52(3)**:97–113.

38. Thomas, M.B. (2003). Introduction to geophysical exploration: magnetic notes on main magnetic field (available at http://www.-galitzin.mines.edu/…/notes).

39. Thompson, D.T. (1982). EULDPH: A new technique for making computer-assisted depth estimates from magnetic data. *Geophysic*s **47**:31-37.

40. Tsegaye Abebe, Manetti, P., Bonini, M., Corti, G., Innocenti, F. and Mazzarini, F. (2005). *Geological Map of the Northern Main Ethiopian Rift*. The Geological Society of America, USA.